Journal of Molecular Spectroscopy **210,** 18–27 (2001)
doi:10.1006/jmsp.2001.8433, available online at http://www.idealibrary.com on IDEAL®

High-Resolution Fourier Transform Spectrum of D_2O in the Region Near 0.97 μm

O. N. Ulenikov,* Shui-Ming Hu,† E. S. Bekhtereva,* G. A. Onopenko,* Sheng-Gui He,† Xiang-Huai Wang,† Jing-Jing Zheng,† and Qing-Shi Zhu†

*Laboratory of Molecular Spectroscopy, Physics Department, Tomsk State University, Tomsk, 634050, Russia; and †Open Research Laboratory of Bond-Selective Chemistry, University of Science and Technology of China, Hefei, 230026, People's Republic of China

E-mail: Ulenikov@phys.tsu.ru; smhu@ustc.edu.cn

Received May 17, 2001; in revised form August 6, 2001; published online October 5, 2001

The high-resolution Fourier transform spectrum of the D_2O molecule were recorded and analyzed in the region near 0.97 μm (10 200–10 440 cm^{-1}) where the bands of the $v = 4$ ($v = v_1 + v_2/2 + v_3$) polyad are located. Transitions belonging to the strongest band of the polyad, $3\nu_1 + \nu_3$, are assigned up to the value of the rotational angular momentum quantum number $J = 13$. The presence of strong local resonance interactions allowed us to assign some transitions to the very weak band $4\nu_1$. Upper states energies obtained on that basis were fitted with a Hamiltonian model which took into account resonance interactions between the states of the $v = 4$ polyad. The derived spectroscopic parameters reproduce the overwhelming majority of assigned transitions within experimental accuracy.

Key Words: vibration–rotation spectra; D_2O molecule; spectroscopic parameters.

1. INTRODUCTION

The H_2O molecule together with its "daughter" deuterated species, HDO and D_2O, is a subject of great interest because of its important role in many problems. In this respect, the investigation of dynamics of molecular vibrations and rotations, determination of intramolecular potential function and study of effects and appearances of intermolecular interactions, studies of planetary atmospheres and of the role of deuterium in interstellar molecules as an indicator of chemical reactions, investigation of industrial pollution, laser engineering, *etc.*, can be mentioned.

The D_2O molecule has been a subject of extensive spectroscopic study during last 30–40 years both in the microwave, and, especially, in the infrared regions (a short review of earlier studies of D_2O spectra can be found in Ref. (*1*)). The present contribution, a part of our systematic investigations of the infrared spectra of deuterated species of the H_2O molecule, (*1–6*), is devoted to the study of the spectral region near 0.97 μm (10 200–10 440 cm^{-1}) where the previously unstudied $3\nu_1 + \nu_3$ absorption band is located. Section 2 of the present contribution presents the details of our experimental part of the study. The Hamiltonian model which is used in the theoretical analysis of the recorded spectrum is considered in Section 3. The results of analysis and discussion are presented in Section 4.

2. EXPERIMENTAL DETAILS

The spectrum was recorded at room temperature with a Bruker IFS 120HR Fourier-transform spectrometer (Hefei) equipped with a multipass gas cell, a tungsten source, a CaF_2 beamsplitter, and a Si-diode detector. The sample of D_2O was purchased from PeKing Chemical Industry, Ltd. (China). The stated abundance of deuterium was 99.8%. In order to identify D_2O lines from HDO and H_2O lines in the same spectral region, two spectra were recorded, one with a "pure" D_2O sample, and another with a 1 : 1 mixture of D_2O and H_2O. The gas pressure and optical path length for the first sample was 2352 Pa and 105 m, respectively, while the corresponding values for the second sample were 1070 Pa and 15 m. The sample cell was not predeuterated when we recorded the first spectrum; thus some lines of HDO and H_2O can also be found easily in that spectrum.

The unapodized resolution, which is defined as 0.9/MOPD (Maximal Optical Path Difference), was 0.02 cm^{-1}, and the Blackman–Harris 3-term apodization function was used.

The line positions were calibrated with those of the H_2O absorptions in this region from the GEISA97 data base. The accuracy of the positions of unblended lines was estimated to be about 0.002–0.004 cm^{-1}. For illustration, small parts of the recorded spectra are presented in Figs. 1 and 2.

3. HAMILTONIAN MODEL AND INITIAL APPROXIMATION FOR THE PARAMETERS

The absorption of D_2O in the 0.97-μm region is caused primarily by the $3\nu_1 + \nu_3$ band. At the same time, because the (301) state belongs to the $v = 4$ polyad of interacting vibrational states, its rovibrational energy levels can be strongly shifted by the other states of the polyad. This means that the Hamiltonian

0022-2852/01 $35.00

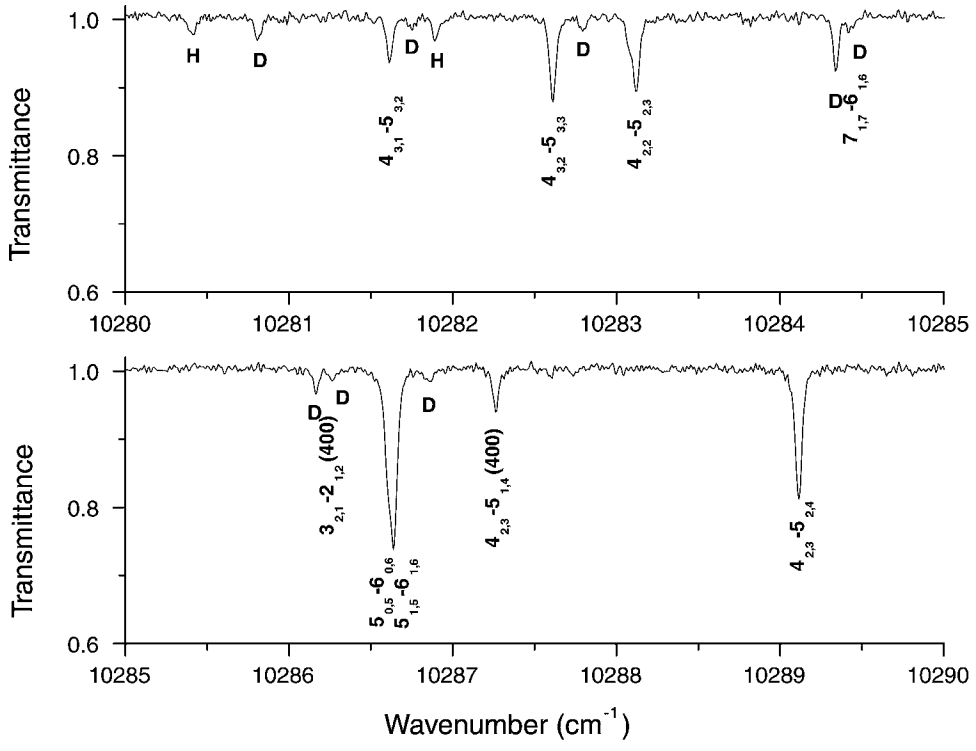

FIG. 1. D_2O transitions in the region 10 280–10 290 cm^{-1}. Assignments of D_2O are given; lines marked by "D" and "H" belong to HDO and H_2O, respectively. See text for experimental details.

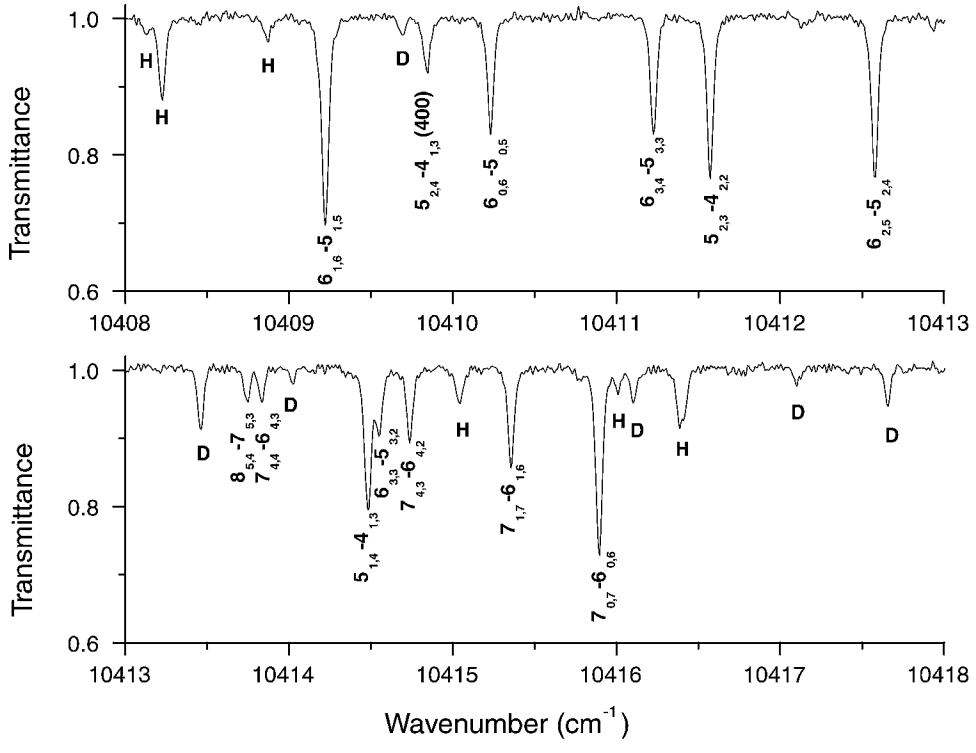

FIG. 2. D_2O transitions in the region 10 408–10 418 cm^{-1}. Assignments of D_2O are given; lines marked by "D" and "H" belong to HDO and H_2O, respectively. See text for experimental details.

model of an isolated vibrational state is not suitable for a study of the rotational structure of the (301) state.

The $v = 4$ polyad consists of 15 vibrational states, (400), (301), (202), (103), (004), (320), (221), (122), (023), (240), (141), (042), (160), (061), and (080), all of which are connected with each other by different types of resonance interactions. The states $(v_1 0 v_3)$ (v_1, $v_3 = 0, 1, 2, 3, 4$) are connected most strongly both with each other and with the nearby $(v_1 2 v_3)$ (v_1, $v_3 = 0$, 1, 2, 3) states. The states $(v_1 4 v_3)$ (v_1, $v_3 = 0$, 1, 2) and, moreover, the $(v_1 6 v_3)$ (v_1, $v_3 = 0$, 1) and (0 8 0) states (1) are located far from the $(v_1 0 v_3)$ states, as can be seen in Fig. 3, and (2) are connected with the $(v_1 0 v_3)$ states only indirectly, by means of the $(v_1 2 v_3)$ states. The above discussion means that (a) all the states $(v_1 0 v_3)$ and $(v_1 2 v_3)$ must be taken into account, while (b) the states $(v_1 4 v_3)$, $(v_1 6 v_3)$, and (080) may be omitted from consideration in the analysis of the rovibrational structure of the (301) vibrational state. As the first step in the theoretical description of the rovibrational energies obtained from the experimental data, we adopted the Hamiltonian model

$$H^{eff.} = \sum_{vv'} |v\rangle\langle v'| H^{vv'}, \qquad [1]$$

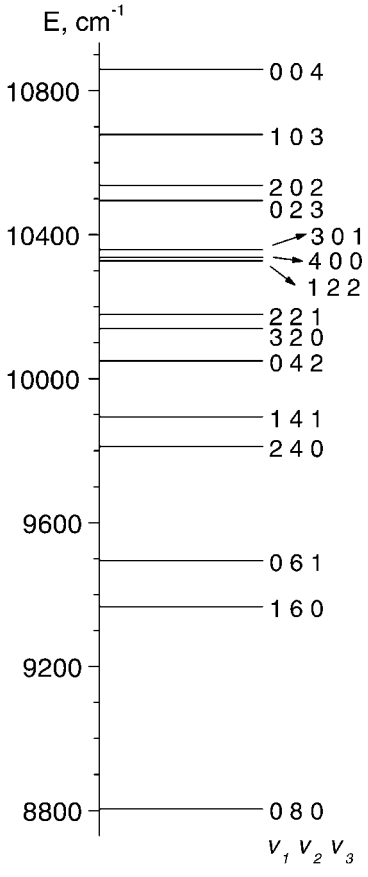

FIG. 3. Illustration of the vibrational energy levels belonging to the $v = 4$ polyad of D_2O.

where $v, v' = 1, \ldots, 9$; $|1\rangle = (320)$, $|2\rangle = (122)$, $|3\rangle = (400)$, $|4\rangle = (202)$, $|5\rangle = (004)$, $|6\rangle = (221)$, $|7\rangle = (301)$, $|8\rangle = (023)$, and $|9\rangle = (103)$. The diagonal operators H^{vv} ($v = 1, \ldots, 9$) are the usual Watson's rotational operators in Ref. (*7*):

$$\begin{aligned} H^{vv} = {} & E^v + \left[A^v - \frac{1}{2}(B^v + C^v)\right] J_z^2 + \frac{1}{2}(B^v + C^v) J^2 \\ & + \frac{1}{2}(B^v - C^v) J_{xy}^2 - \Delta_K^v J_z^4 - \Delta_{JK}^v J_z^2 J^2 - \Delta_J^v J^4 \\ & - \delta_K^v \left[J_z^2, J_{xy}^2\right]_+ - 2\delta_J^v J^2 J_{xy}^2 + H_K^v J_z^6 + H_{KJ}^v J_z^4 J^2 \\ & + H_{JK}^v J_z^2 J^4 + H_J^v J^6 + \left[J_{xy}^2, h_K^v J_z^4 + h_{JK}^v J^2 J_z^2 \right. \\ & \left. + h_J^v J^4\right]_+ + L_K^v J_z^8 + L_{KKJ}^v J_z^6 J^2 + L_{KJ}^v J_z^4 J^4 \\ & + L_{KJJ}^v J_z^2 J^6 + L_J^v J^8 + \left[J_{xy}^2, l_K^v J_z^6 + l_{KJ}^v J^4 J_z^2 \right. \\ & \left. + l_{JK}^v J^2 J_z^4 + l_J^v J^6\right]_+ + P_K^v J_z^{10} + \cdots . \end{aligned} \qquad [2]$$

Operators $H^{vv'}$ ($v \neq v'$) account for the resonance interactions. In this case, since D_2O is an asymmetric top molecule with the symmetry group C_{2v}, its vibrational basis functions $(v_1 v_2 v_3)$ with even values of v_3 have the symmetry A_1, and functions with odd values of v_3 have the symmetry B_1. As the consequence, two types of resonance operators $H^{vv'}$ ($v \neq v'$) may be presented in the Hamiltonian [1]:

(a) Fermi-type resonance interactions which connect vibrational states of the same symmetry are described by the operators

$$\begin{aligned} H^{vv'} = {} & F_0^{vv'} + F_K^{vv'} J_z^2 + F_J^{vv'} J^2 + F_{JJ}^{vv'} J^4 + \cdots \\ & + F_{xy}^{vv'} J_{xy}^2 + F_{xyK}^{vv'} \left[J_{xy}^2, J_z^2\right]_+ + F_{xyJ}^{vv'} J_{xy}^2 J^2 \\ & + F_{xyJK}^{vv'} J^2 \left[J_{xy}^2, J_z^2\right]_+ + F_{xyJJ}^{vv'} J_{xy}^2 J^4 + \cdots . \end{aligned} \qquad [3]$$

(b) Coriolis-type interactions which connect states of different symmetries are described by the operators

$$\begin{aligned} H^{vv'} = {} & C_y^{vv'} i J_y + \cdots + C_{xz}^{vv'} [J_x, J_z]_+ + C_{xzK}^{vv'} \left[[J_x, J_z]_+, J_z^2\right]_+ \\ & + C_{xzJ}^{vv'} [J_x, J_z]_+ J^2 + C_{xzKK}^{vv'} \left[[J_x, J_z]_+, J_z^4\right]_+ \\ & + C_{xzJK}^{vv'} J^2 \left[[J_x, J_z]_+, J_z^2\right]_+ + \cdots + C_{yxy}^{vv'} (J_+^3 + J_-^3) \\ & + C_{yxyK}^{vv'} \left[(J_+^3 + J_-^3), J_z^2\right]_+ \cdots . \end{aligned} \qquad [4]$$

In Eqs. [2]–[4] the following notations are used: $J_{xy}^2 = J_x^2 - J_y^2$, $J^2 = \sum_\alpha J_\alpha^2$, $J_\pm = J_x \mp i J_y$, and $[A, B]_+ = AB + BA$.

Of course, both the remaining states of the $v = 4$ polyad and states of other neighboring polyads ($v \neq 4$) may perturb some individual rovibrational levels of the (301) state. However, one may expect that such perturbations will not induce large shifts or affect many levels, and the Hamiltonian described in Eqs. [1]–[4]

will account for the overwhelming majority of possible interactions and peculiarities in the spectrum of the $3\nu_1 + \nu_3$ band.

The presence of numerous resonance interactions between the states of the $v = 4$ polyad makes it actually a problem to estimate the initial values for the rotational and centrifugal distortion coefficients. This problem was solved in the present study in the following way:

(a) The vibrational energies E^v of all the vibrational states of the $v = 4$ polyad were estimated from the fit of the values of band centers of earlier observed polyads of the D_2O molecule: $\nu_2 = 1178.38\ cm^{-1}$ (*8*); $\nu_1 = 2671.65\ cm^{-1}$, $2\nu_2 = 2336.84\ cm^{-1}$, and $\nu_3 = 2787.72\ cm^{-1}$ (*9*); $\nu_1 + \nu_2 = 3841.42\ cm^{-1}$, $\nu_2 + \nu_3 = 3956.01\ cm^{-1}$, and $3\nu_2 = 3474.32\ cm^{-1}$ (*2*); $2\nu_1 = 5291.72\ cm^{-1}$, $\nu_1 + \nu_3 = 5373.90\ cm^{-1}$, $2\nu_3 = 5529.44\ cm^{-1}$, $\nu_1 + 2\nu_2 = 4990.83\ cm^{-1}$, and $2\nu_2 + \nu_3 = 5105.38\ cm^{-1}$ (*1*); $2\nu_1 + \nu_2 = 6452.98\ cm^{-1}$, $\nu_1 + \nu_2 + \nu_3 = 6533.24\ cm^{-1}$, $\nu_2 + 2\nu_3 = 6687.00\ cm^{-1}$, $\nu_1 + 3\nu_2 = 6119.04\ cm^{-1}$ and $3\nu_2 + \nu_3 = 6235.08\ cm^{-1}$ (*10*); $3\nu_1 = 7852.93\ cm^{-1}$, $2\nu_1 + \nu_3 = 7899.82\ cm^{-1}$, $\nu_1 + 2\nu_3 = 8054.06\ cm^{-1}$, $3\nu_3 = 8220.18\ cm^{-1}$, $2\nu_1 + 2\nu_2 = 7593.12\ cm^{-1}$, $\nu_1 + 2\nu_2 + \nu_3 = 7672.92\ cm^{-1}$, and $2\nu_2 + 2\nu_3 = 7825.37\ cm^{-1}$ (*4*); $3\nu_1 + \nu_2 = 9005.35\ cm^{-1}$, $2\nu_1 + \nu_2 + \nu_3 = 9050.36\ cm^{-1}$, $\nu_1 + \nu_2 + 2\nu_3 = 9201.90\ cm^{-1}$, $3\nu_1 + 2\nu_3 = 8934.60\ cm^{-1}$, and $\nu_1 + 3\nu_2 + \nu_3 = 8788.60\ cm^{-1}$(*5*). The values of the ω_λ, $x_{\lambda\mu}$, $F_0^{F\cdot}$, and $F_0^{D.-D.}$ parameters derived from discussed fit (the last are the Fermi and Darling–Dennison interaction constants) then were used in estimation of the band centers of the ($v = 4$) polyad. Obtained on that way band centers, which are denoted as E, are presented in the first line of Table 1. Figure 3 shows the relative positions of the vibrational energy levels belonging to the $v = 4$ polyad.

(b) The rotational parameters A^v, B^v, and C^v of the (320), (122), (400), (202), (004), (221), (301), (023), and (103) vibrational states were estimated by the simple equation

$$P^{v_1 v_2 v_3} = P^{0 v_2 0} + v_1(P^{100} - P^{000}) + v_3(P^{001} - P^{000}), \quad [5]$$

where P denotes any of the parameters A^v, B^v, or C^v; the values of the parameters of the (000), (100), (001), and (020) vibrational states were taken from (*8*) and (*9*).

(c) All the values of the centrifugal distortion coefficients of the ($v_1 0 v_3$) and ($v_1 2 v_3$) vibrational states were taken to be equal to the values of corresponding coefficients of the (000) and (020) states, (*9*), respectively.

(d) All the initial values of Coriolis type parameters were set to zero.

4. ANALYSIS AND DISCUSSION

The observed transitions were assigned using the ground state combination differences method, and the ground state rotational energies were calculated on the basis of the parameters from Ref. (*9*). As a result of the analysis, we assigned 184 transitions

TABLE 1
Adjusted Final Spectroscopic Parameters of the (400), (301), (202), (221), (122), and (023) Vibrational States of the D_2O Molecule (in cm^{-1})[a]

Parameter	(400)	(301)	(202)	(221)	(122)	(023)
E	10337.11	10358.56086(217)	10537.56	10178.36	10327.84	10495.11
A	14.400	14.188765(634)	13.874	17.130	17.52341(676)	16.544
B	7.05452(258)	6.985060(458)	7.031	7.188	7.198(285)	7.318
C	4.614	4.53336(269)	4.611	4.562	4.570	4.578
$\Delta_K \times 10^3$	9.25347	7.9211(401)	9.25347	21.986	21.986	21.986
$\Delta_{JK} \times 10^3$	−1.52324	−1.52324	−1.52324	−2.368	−2.368	−2.368
$\Delta_J \times 10^3$	0.309983	0.35783(769)	0.309983	0.3682	0.3682	0.3682
$\delta_K \times 10^3$	0.34708	0.34708	0.34708	1.3004	1.3004	1.3004
$\delta_J \times 10^3$	0.123109	0.09623(486)	0.123109	0.1531	0.1531	0.1531
$H_K \times 10^5$	1.8449	1.8449	1.8449	8.80	8.80	8.80
$H_{KJ} \times 10^5$	−0.2457	−0.2457	−0.2457	−0.629	−0.629	−0.629
$H_{JK} \times 10^5$	−0.02149	−0.02149	−0.02149	—	—	—
$H_J \times 10^5$	0.006513	0.006513	0.006513	0.0106	0.0106	0.0106
$h_K \times 10^5$	0.3790	0.3790	0.3790	1.073	1.073	1.073
$h_{JK} \times 10^5$	−0.00528	−0.00528	−0.00528	—	—	—
$h_J \times 10^5$	0.003226	0.003226	0.003226	0.00518	0.00518	0.00518
$L_K \times 10^7$	−0.5964	−0.5964	−0.5964	−3.01	−3.01	−3.01
$L_{KKJ} \times 10^7$	0.151	0.151	0.151	—	—	—
$L_{KJ} \times 10^7$	0.0384	0.0384	0.0384	—	—	—
$L_{KJJ} \times 10^7$	0.00054	0.00054	0.00054	—	—	—
$L_J \times 10^7$	−0.000168	−0.000168	−0.000168	—	—	—
$l_K \times 10^7$	−0.173	−0.173	−0.173	—	—	—
$l_J \times 10^7$	−0.0000836	−0.0000836	−0.0000836	—	—	—
$P_K \times 10^9$	0.1516	0.1516	0.1516	—	—	—

[a] Values in parentheses are the 1σ statistical confidence intervals. Parameters presented without confidence intervals were fixed and not fitted (see text for details).

TABLE 2
The Assigned Rovibrational Transitions of D_2O

Upper state			Lower state				Line position,	Line position,	$\delta^a \times 10^3$,
J'	K'_a	K'_c	J	K_a	K_c	Band	exp./cm^{-1}	calc./cm^{-1}	/cm^{-1}
1			2			3	4	5	6
9	4	5	10	4	6	301	10189.515	10189.516	−1
11	0	11	12	0	12	301	10202.079	10202.072	7
10	2	9	11	2	10	301	10202.782	10202.782	0
8	5	4	9	5	5	301	10203.062	10203.069	−7
10	1	9	11	1	10	301	10203.293	10203.292	1
7	7	0	8	7	1	301	10204.208	10204.208	0
7	7	1	8	7	2	301	10204.208	10204.208	0
8	4	4	9	4	5	301	10208.483	10208.470	13
8	3	5	9	3	6	301	10211.023	10211.022	1
7	6	2	8	6	3	301	10212.365	10212.371	−6
7	6	1	8	6	2	301	10212.365	10212.367	−2
10	0	10	11	0	11	301	10217.353	10217.350	3
10	1	10	11	1	11	301	10217.353	10217.352	1
9	2	8	10	2	9	301	10217.766	10217.776	−10
9	1	8	10	1	9	301	10218.472	10218.481	−9
8	3	6	9	3	7	301	10219.571	10219.571	0
7	5	3	8	5	4	301	10220.536	10220.542	−6
7	5	2	8	5	3	301	10220.536	10220.539	−3
7	4	3	8	4	4	301	10226.688	10226.683	5
6	6	1	7	6	2	301	10229.274	10229.274	0
6	6	0	7	6	1	301	10229.274	10229.273	1
7	3	4	8	3	5	301	10229.430	10229.431	−1
7	2	5	8	2	6	301	10231.534	10231.538	−4
9	0	9	10	0	10	301	10232.192	10232.201	−9
9	1	9	10	1	10	301	10232.192	10232.184	8
8	2	7	9	2	8	301	10232.385	10232.389	−4
8	1	7	9	1	8	301	10233.275	10233.276	−1
7	3	5	8	3	6	301	10235.627	10235.612	15
6	5	2	7	5	3	301	10237.409	10237.417	−8
6	5	1	7	5	2	301	10237.409	10237.375	34
6	4	2	7	4	3	301	10244.125	10244.133	−8
6	4	3	7	4	4	301	10244.648	10244.649	−1
8	1	8	9	1	9	301	10246.497	10246.491	6
8	0	8	9	0	9	301	10246.538	10246.540	−2
7	2	6	8	2	7	301	10246.722	10246.721	1
7	1	6	8	1	7	301	10247.708	10247.700	8
6	3	3	7	3	4	301	10247.505	10247.498	7
6	2	4	7	2	5	301	10249.427	10249.418	9
6	3	4	7	3	5	301	10251.563	10251.552	9
9	1	9	9	1	8	301	10253.290	10253.279	11
5	5	1	6	5	2	301	10253.711	10253.716	−5
5	5	0	6	5	1	301	10253.711	10253.710	1
7	1	7	8	1	8	301	10260.326	10260.328	−2
7	0	7	8	0	8	301	10260.398	10260.402	−4
5	4	1	6	4	2	301	10260.719	10260.727	−8
5	4	2	6	4	3	301	10260.901	10260.903	−2
6	2	5	7	2	6	301	10260.901	10260.904	−3
6	1	5	7	1	6	301	10261.834	10261.831	3
5	3	2	6	3	3	301	10264.997	10265.001	−4
5	2	3	6	2	4	301	10266.486	10266.488	−2
5	3	3	6	3	4	301	10267.256	10267.257	−1
5	2	4	6	1	5	400	10271.369	10271.370	−1
6	1	6	7	1	7	301	10273.701	10273.690	11

[a] The δ is the difference between experimental and calculated values of line position.

TABLE 2—*Continued*

Upper state			Lower state						
J'	K'_a	K'_c	J	K_a	K_c	Band	Line position, exp./cm^{-1}	Line position, calc./cm^{-1}	$\delta^a \times 10^3$, /cm^{-1}
1			2			3	4	5	6
6	0	6	7	0	7	301	10273.773	10273.776	−3
5	2	4	6	2	5	301	10275.032	10275.035	−3
5	1	4	6	1	5	301	10276.007	10276.012	−5
4	4	0	5	4	1	301	10276.535	10276.527	8
4	4	1	5	4	2	301	10276.575	10276.571	4
4	3	1	5	3	2	301	10281.614	10281.617	−3
4	3	2	5	3	3	301	10282.614	10282.613	1
4	2	2	5	2	3	301	10283.124	10283.130	−6
7	1	7	7	1	6	301	10284.420	10284.424	−4
5	0	5	6	0	6	301	10286.638	10286.641	−3
4	1	3	5	1	4	301	10287.267	10287.263	4
5	1	4	5	3	3	301	10288.046	10288.047	−1
4	2	3	5	2	4	301	10289.117	10289.115	2
4	2	3	5	1	4	400	10290.982	10290.982	0
3	3	0	4	3	1	301	10297.191	10297.187	4
3	3	1	4	3	2	301	10297.516	10297.506	10
3	2	2	4	1	3	400	10298.524	10298.521	3
4	0	4	5	0	5	301	10298.972	10298.972	0
4	1	4	5	1	5	301	10299.110	10299.107	3
3	2	1	4	2	2	301	10299.403	10299.404	−1
6	1	6	6	1	5	301	10299.905	10299.892	13
3	1	2	4	1	3	301	10302.469	10302.467	2
3	2	2	4	2	3	301	10303.059	10303.052	7
8	6	2	8	6	3	301	10306.256	10306.242	14
8	6	3	8	6	2	301	10306.256	10306.284	−28
3	3	3	4	0	4	301	10310.835	10310.829	6
7	6	1	7	6	2	301	10311.238	10311.236	2
7	6	2	7	6	3	301	10311.238	10311.236	2
3	1	3	4	1	4	301	10311.314	10311.316	−2
8	3	6	8	3	5	301	10311.903	10311.905	−2
8	5	4	8	5	3	301	10314.541	10314.542	−1
2	2	0	3	2	1	301	10315.027	10315.023	4
2	1	1	3	1	2	301	10315.255	10315.257	−2
6	6	1	6	6	0	301	10315.718	10315.716	2
6	6	0	6	6	1	301	10315.718	10315.716	2
2	2	1	3	2	2	301	10316.723	10316.723	0
2	2	1	3	1	2	400	10317.438	10317.439	−1
7	5	2	7	5	3	301	10319.747	10319.744	3
6	2	5	6	2	4	301	10320.896	10320.905	−9
2	0	2	3	0	3	301	10322.495	10322.490	5
2	1	2	3	1	3	301	10323.341	10323.343	−2
6	5	1	6	5	2	301	10323.933	10323.945	−12
7	3	5	7	3	4	301	10324.168	10324.160	8
8	4	4	8	4	5	301	10325.438	10325.422	16
7	4	4	7	4	3	301	10326.233	10326.233	0
5	5	1	5	5	0	301	10327.771	10327.768	3
5	5	0	5	5	1	301	10327.771	10327.768	3
7	4	3	7	4	4	301	10328.251	10328.248	3
1	1	0	2	1	1	301	10330.387	10330.388	−1
6	4	3	6	4	2	301	10331.136	10331.139	−3
2	2	0	3	1	3	400	10331.722	10331.714	8
5	2	4	5	2	3	301	10333.134	10333.137	−3
6	3	4	6	3	3	301	10333.313	10333.303	10
1	0	1	2	0	2	301	10334.331	10334.331	0
5	4	2	5	4	1	301	10335.062	10335.063	−1
5	4	1	5	4	2	301	10335.184	10335.186	−2
1	1	1	2	1	2	301	10335.240	10335.243	−3

TABLE 2—*Continued*

Upper state			Lower state				Line position, exp./cm^{-1}	Line position, calc./cm^{-1}	$\delta^a \times 10^3$, /cm^{-1}
J'	K'_a	K'_c	J	K_a	K_c	Band			
1			2			3	4	5	6
4	4	1	4	4	0	301	10338.274	10338.261	13
4	4	0	4	4	1	301	10338.274	10338.275	−1
5	3	3	5	3	2	301	10339.640	10339.636	4
6	3	3	6	3	4	301	10342.172	10342.169	3
4	2	3	4	2	2	301	10342.526	10342.523	3
5	3	2	5	3	3	301	10342.918	10342.917	1
4	3	2	4	3	1	301	10343.868	10343.867	1
4	3	1	4	3	2	301	10344.740	10344.740	0
0	0	0	1	0	1	301	10346.446	10346.444	2
3	3	1	3	3	0	301	10346.736	10346.729	7
3	3	0	3	3	1	301	10346.863	10346.858	5
2	1	2	2	1	1	301	10348.506	10348.510	−4
3	2	2	3	2	1	301	10348.913	10348.911	2
2	2	1	2	2	0	301	10352.620	10352.615	5
3	2	1	3	2	2	301	10353.549	10353.548	1
2	2	0	2	2	1	301	10353.600	10353.598	2
1	1	1	1	1	0	301	10354.625	10354.628	−3
4	2	2	4	2	3	301	10355.009	10355.011	−2
5	2	3	5	2	4	301	10358.165	10358.168	−3
1	1	0	1	1	1	301	10359.468	10359.468	0
2	1	1	2	1	2	301	10362.162	10362.159	3
6	2	4	6	2	5	301	10362.611	10362.586	25
2	2	1	2	1	2	400	10364.343	10364.341	2
3	2	2	3	1	3	400	10365.108	10365.101	7
3	1	2	3	1	3	301	10369.048	10369.048	0
1	0	1	0	0	0	301	10370.212	10370.209	3
4	1	3	4	1	4	301	10374.890	10374.889	1
2	1	2	1	1	1	301	10377.589	10377.591	−2
2	0	2	1	0	1	301	10380.827	10380.820	7
2	1	1	1	1	0	301	10381.548	10381.544	−4
2	2	1	1	1	0	400	10383.727	10383.726	1
2	2	0	1	1	1	400	10385.962	10385.962	0
3	1	3	2	1	2	301	10386.555	10386.559	−4
3	2	2	2	2	1	301	10387.492	10387.486	6
3	2	1	2	2	0	301	10389.441	10389.440	1
3	0	3	2	0	2	301	10389.944	10389.938	6
3	2	2	2	1	1	400	10390.274	10390.268	6
4	2	3	4	0	4	301	10391.720	10391.714	6
4	3	2	3	3	1	301	10393.539	10393.537	2
4	3	1	3	3	0	301	10393.958	10393.963	−5
3	1	2	2	1	1	301	10394.218	10394.215	3
4	1	4	3	1	3	301	10394.846	10394.844	2
4	2	3	3	2	2	301	10396.668	10396.667	1
5	4	2	4	4	1	301	10396.808	10396.810	−2
5	4	1	4	4	0	301	10396.878	10396.877	1
4	0	4	3	0	3	301	10397.562	10397.563	−1
7	6	1	6	6	0	301	10397.679	10397.679	0
7	6	2	6	6	1	301	10397.679	10397.679	0
6	5	2	5	5	1	301	10398.002	10398.005	−3
6	5	1	5	5	0	301	10398.002	10397.997	5
6	3	4	6	1	5	301	10399.197	10399.185	12
7	1	6	7	1	7	301	10399.764	10399.756	8
4	2	2	3	2	1	301	10400.866	10400.870	−4
5	1	5	4	1	4	301	10402.401	10402.391	10
5	3	3	4	3	2	301	10402.761	10402.759	2
4	1	3	3	1	2	301	10403.233	10403.230	3
5	0	5	4	0	4	301	10404.175	10404.171	4

TABLE 2—*Continued*

Upper state			Lower state				Line position, exp./cm^{-1}	Line position, calc./cm^{-1}	$\delta^a \times 10^3$, /cm^{-1}
J'	K'_a	K'_c	J	K_a	K_c	Band			
1			2			3	4	5	6
5	3	2	4	3	1	301	10404.175	10404.176	−1
5	2	4	4	2	3	301	10405.014	10405.018	−4
8	6	2	7	6	1	301	10405.127	10405.106	21
8	6	3	7	6	2	301	10405.127	10405.154	−27
6	4	3	5	4	2	301	10405.597	10405.599	−2
6	4	2	5	4	1	301	10405.887	10405.890	−3
8	1	7	8	1	8	301	10405.887	10405.887	0
7	5	2	6	5	1	301	10406.274	10406.274	0
4	2	3	3	1	2	400	10406.952	10406.949	3
6	1	6	5	1	5	301	10409.223	10409.214	9
5	2	4	4	1	3	400	10409.848	10409.848	0
6	0	6	5	0	5	301	10410.232	10410.233	−1
6	3	4	5	3	3	301	10411.227	10411.219	−8
9	1	8	9	1	9	301	10411.227	10411.221	−6
5	2	3	4	2	2	301	10411.574	10411.576	−2
6	2	5	5	2	4	301	10412.581	10412.585	−4
8	5	4	7	5	3	301	10413.752	10413.748	4
7	4	4	6	4	3	301	10413.837	10413.830	7
5	1	4	4	1	3	301	10414.486	10414.490	−4
6	3	3	5	3	2	301	10414.553	10414.548	5
7	4	3	6	4	2	301	10414.739	10414.738	1
7	1	7	6	1	6	301	10415.358	10415.365	−7
7	0	7	6	0	6	301	10415.895	10415.899	−4
7	3	5	6	3	4	301	10418.846	10418.832	14
7	2	6	6	2	5	301	10419.394	10419.393	1
6	2	4	5	2	3	301	10420.705	10420.689	16
8	1	8	7	1	7	301	10420.911	10420.904	7
8	0	8	7	0	7	301	10421.169	10421.171	−2
8	4	4	7	4	3	301	10423.772	10423.760	12
7	3	4	6	3	3	301	10424.862	10424.867	−5
8	2	7	7	2	6	301	10425.439	10425.440	−1
8	3	6	7	3	5	301	10425.588	10425.589	−1
9	1	9	8	1	8	301	10425.898	10425.890	8
9	0	9	8	0	8	301	10425.986	10426.005	−19
7	2	5	6	2	4	301	10427.321	10427.322	−1
8	1	7	7	1	6	301	10429.990	10429.983	7
10	1	10	9	1	9	301	10430.293	10430.292	1
10	0	10	9	0	9	301	10430.342	10430.335	7
9	2	8	8	2	7	301	10430.726	10430.728	−2
9	3	7	8	3	6	301	10431.515	10431.515	0
9	4	5	8	4	4	301	10432.979	10432.981	−2
9	1	8	8	1	7	301	10433.574	10433.578	−4
11	0	11	10	0	10	301	10434.224	10434.222	2
8	3	5	7	3	4	301	10434.381	10434.380	1
10	2	9	9	2	8	301	10435.301	10435.294	7
10	1	9	9	1	8	301	10436.972	10436.971	1
12	0	12	11	0	11	301	10437.578	10437.580	−2
12	1	12	11	1	11	301	10437.578	10437.561	17
11	2	10	10	2	9	301	10439.047	10439.055	−8
13	0	13	12	0	12	301	10440.476	10440.480	−4
13	1	13	12	1	12	301	10440.476	10440.469	7

TABLE 3
Parameters of Resonance Interactions (in cm^{-1}) Between Some States of the $v = 4$ Polyad of D_2O[a]

Parameter	Value	Parameter	Value	Parameter	Value
		Fermi Type Interactions			
$F_0^{122,400}$	−6.706(857)	$F_K^{122,400}$	1.1549(201)	$F_{xy}^{122,400}$	0.11214(288)
$F_{xyJ}^{122,400}10^2$	−0.09278(325)	$F_K^{221,301}$	−0.36209(492)	$F_{JJ}^{221,301}10^2$	0.093740(270)
$F_{xy}^{221,301}$	0.1389(119)	$F_{xyK}^{221,301}10^2$	−0.4964(390)	$F_{xyJ}^{221,301}10^2$	−0.2945(192)
$F_{xyJJ}^{221,301}10^4$	−0.5872(486)	$F_{xyJK}^{221,301}10^4$	−0.09506(888)	$F_{xy}^{023,301}$	−0.01160(175)
		Coriolis Type Interactions			
$C_y^{122,301}$	−0.20478(695)	$C_{xz}^{122,301}$	0.13004(387)	$C_y^{400,301}$	1.0347(216)
$C_{xz}^{400,301}$	−0.09981(738)	$C_{xzJ}^{400,301}10^2$	0.03710(566)	$C_{xzJ}^{202,301}10^2$	−0.4333(164)
$C_{xzKK}^{202,301}10^4$	−2.0418(909)	$C_{xzJK}^{202,301}10^4$	1.7332(649)	$C_{yxy}^{202,301}10^2$	0.8811(480)
		$C_{yxyK}^{202,301}10^4$	−3.250(168)		

[a] Values in parentheses are 1σ statistical confidence intervals.

with $J^{max.} = 13$ and $K_a^{max.} = 7$ to the $3\nu_1 + \nu_3$ band. A list of assigned transitions is presented in Table 2. Because the (301) state is strongly perturbed by other states of the $v = 4$ polyad, one can expect the appearance in the recorded spectrum of some transitions belonging to the corresponding weak bands. Indeed, we assigned without doubt 12 transitions to the $4\nu_1$ band. They are also presented in Table 2.

As was mentioned above, the (301) state interacts strongly with practically all the states $(\upsilon_1 0 \upsilon_3)$ and $(\upsilon_1 2 \upsilon_3)$ of the $v = 4$ polyad. The strongest interactions were found not only between the state (301) and its nearest neighbors, (400) and (122) (see Fig. 3 and Table 1), but also between the (301) and the (221), (202) states.

In the first step of the analysis, the set of levels $E_{[J0J](301)}$ was fitted. As the result of the fit, 14 levels were correctly reproduced by four parameters E, B, C, and Δ_K. However, an attempt to add more of the sets of energies $E_{[J1J](301)}$ into the fit procedure did not allow us to reproduce the initial data accurately even with an addition of either six or seven extra parameters of the (301) state, or Coriolis interaction coefficients of the type $C^{301,400}$ or $C^{301,122}$. The reason lies in the presence of strong local interactions between the (301) state and the (023), (221) states.

Analogous analysis showed that the (301) state is directly connected by strong local resonance interactions with the (400), (122), (202), (023), and, especially, (221) vibrational states. At the same time, it was found that three other vibrational states, (103), (004), and (320), of the $v = 4$ polyad, which were taken into consideration in the first step of the analysis, may be omitted because their influence on the fitted rovibrational energies in our study is small. For this reason, in the final fit we used the Hamiltonian model [1]–[4] with six interacting vibrational states: (122), (400), (202), (221), (301), and (023). The parameters obtained from the fit are presented in Tables 1 and 3 together with their 1σ statistical confidence intervals. Those parameters presented in Table 1 without confidence intervals were fixed to their values theoretically estimated on the base of points (*a*)–(*c*) (see last paragraph of Section 3). If one takes into account the presence of numerous resonance interactions and practically total absence of any regularity in the rovibrational structure of the (301) state, the number of 32 fitted parameters is not looked as unsuitably large. In this case the question can be asked: why we did not use the Watson's Hamiltonian, but with a Padé-type summing up procedure? The answer is: the efficiency of the Padé-approximation strongly depends on the "quality" of initial experimental data which are used in a fit. Namely, the more numerous the values of the quantum numbers J, K_a, and υ_2 of the fitted states of the H_2O, D_2O, or HDO molecule, the more efficient the use of Padé-type procedures in comparison with Watson's Hamiltonian. In our case, on the one hand, the quantum number υ_2 equals zero for the $3\nu_1 + \nu_3$ band analyzed in the present study and, on the other hand, upper energies with only not large values of quantum numbers J and K_a ($J^{max.} = 13$ and $K_a^{max.} = 7$) were obtained from experimental data and used in the fit. So one can expect (and this really was confirmed in our corresponding attempt to fit the "experimental" energies with the Padé-type Hamiltonian) that the using of the Padé summing will not reduce the number of fitted parameters.

The values of the fitted rotational parameters and centrifugal distortion coefficients of the (301), (400), and (122) states seem to be physically meaningful because they are very close to the values of corresponding parameters of the (000) or (020) states. The ability of derived parameters to reproduce the spectrum can be seen from columns 5 and 6 of Table 2 which present the values $\nu^{calc.}$ and $\delta = \nu^{exp.} - \nu^{calc.}$, respectively ($\nu^{exp.}$ is the experimentally recorded line position, and $\nu^{calc.}$ is its value calculated with the parameters from Tables 1 and 3). One can see that the majority of the line positions are reproduced with deviations not far from the experimental uncertainties (the lasts were estimated to

be 0.002–0.004 cm^{-1} for unblended and not very weak lines; experimental uncertainties for weak lines may be increased up to 0.015–0.020 cm^{-1}).

ACKNOWLEDGMENTS

This work was partially supported by the National Project for the Development of Key Fundamental Sciences in China, by the National Natural Science Foundation of China, by the Foundation of the Chinese Academy of Science, and by the Ministry of Education of Russian Federation. O. Ulenikov thanks the University of Science and Technology of China for a guest professorship.

REFERENCES

1. X.-H. Wang, O. N. Ulenikov, G. A. Onopenko, E. S. Bekhtereva, S.-G. He, S.-M. Hu, H. Lin, and Q.-S. Zhu, *J. Mol. Spectrosc.* **200,** 25–33 (2000).
2. S.-G. He, O. N. Ulenikov, G. A. Onopenko, E. S. Bekhtereva, X.-H. Wang, S.-M. Hu, H. Lin, and Q.-S. Zhu, *J. Mol. Spectrosc.* **200,** 34–39 (2000).
3. S.-M. Hu, O. N. Ulenikov, G. A. Onopenko, E. S. Bekhtereva, S.-G. He, X.-H. Wang, H. Lin, and Q.-S. Zhu, *J. Mol. Spectrosc.* **203,** 228–234 (2000).
4. O. N. Ulenikov, S.-G. He, G. A. Onopenko, E. S. Bekhtereva, X.-H. Wang, S.-M. Hu, H. Lin, and Q.-S. Zhu, *J. Mol. Spectrosc.* **204,** 216–225 (2000).
5. J.-J. Zheng, O. N. Ulenikov, G. A. Onopenko, E. S. Bekhtereva, S.-G. He, X.-H. Wang, S.-M. Hu, H. Lin, and Q.-S. Zhu, *Mol. Phys.* **99,** 931–937 (2001).
6. O. N. Ulenikov, S.-M. Hu, E. S. Bekhtereva, G. A. Onopenko, X.-H. Wang, S.-G. He, J.-J. Zheng, and Q.-S. Zhu, *J. Mol. Spectrosc.* **208,** 224–235 (2001).
7. J. K. G. Watson, *J. Chem. Phys.* **46,** 1935–1949 (1967).
8. C. Camy-Peyret, J.-M. Flaud, A. Mahmoudi, G. Guelachvili, and J. W. C. Johns, *Int. J. Infrared Millimeter Waves* **6,** 199–233 (1985).
9. N. Papineau, J.-M. Flaud, C. Camy-Peyret, and G. Guelachvili, *J. Mol. Spectrosc.* **87,** 219–232 (1981).
10. P. S. Ormsby, K. Narahari Rao, M. Winnewisser, B. P. Winnewisser, O. V. Naumenko, A. D. Bykov, and L. N. Sinitsa, *J. Mol. Spectrosc.* **158,** 109–130 (1993).